

Are Ionic Liquids Really a Boon for the Synthesis of Inorganic Materials? A General Method for the Fabrication of Nanosized Metal Fluorides

David S. Jacob,[†] Liora Bitton,[‡] Judith Grinblat,[†] Israel Felner,[§] Yuri Koltypin,[†] and Aharon Gedanken^{†,*}

Department of Chemistry and Kanbar Laboratory for Nanomaterials at the Bar-Ilan University Center for Advanced Materials and Nanotechnology and Department of Physics, Bar-Ilan University, 52900 Ramat-Gan, Israel, and The Racah Institute of Physics, The Hebrew University of Jerusalem, 91904 Jerusalem, Israel

Received April 4, 2006. Revised Manuscript Received April 28, 2006

This article presents a simple and fast method to synthesize metal fluorides such as FeF₂, CoF₂, ZnF₂, LaF₃, YF₃, SrF₂, and metal oxide Fe₂O₃ having different morphologies. The synthesis is carried out in an ionic liquid solvent using a domestic microwave oven. The products are characterized with the help of an X-ray diffraction method. The different morphologies of the products are studied with the help of a high-resolution transmission electron microscope and a high-resolution scanning electron microscope. The change in the oxidation state of the reactant Fe(III) to the product Fe(II) is confirmed through Mössbauer studies. The presence of carbon and its application as a reducing agent is illustrated by Raman spectroscopy.

Introduction

Strategies for the fabrication of nanomaterials are of fundamental importance in the advancement of science and technology.¹ In the area of nanotechnology, one-dimensional nanometer-sized materials such as nanowires, nanotubes, nanorods, and nanoribbons have attracted considerable attention because of their intrinsic size-dependent properties and resulting applications.^{2–4}

Scientists are always in search of new chemistry and in need of new solvents that have multi-universal properties that can act as templates, have a low vapor pressure, have a high thermal stability, and show high solubility for organic, inorganic, and organometallic compounds. Room-temperature ionic liquids (RTILs) are well-known solvents with the above promising properties and have received much attention in many areas of chemistry and industry.⁵ The use of RTILs is well-documented in important fields such as synthetic-organic chemistry, separation, and electrochemistry.^{6–8} The

importance of RTILs in the field of inorganic nanosynthesis has gradually been realized and is presently the subject of intense research with published reports on the synthesis of nanostructured materials such as platinum, palladium, and rhodium nanoparticles.⁹ Tellurium nanowires were prepared in an ionic liquid (IL) where poly(vinylpyrrolidone) acts as a stabilizer.¹⁰ Ir and Rh nanoparticles were synthesized in ILs by a chemical reduction.¹¹ Anisotropic gold nanoparticles were synthesized in an ionogel template.¹² CoPt nanorods were synthesized in an IL using cetyltrimethylammonium bromide as a surfactant.¹³ LaCo₃OH nanowires were synthesized in an IL.¹⁴ ZnO was formed in an IL with different morphologies under NaOH as a basic medium.^{15,16} Hollow TiO₂ microspheres, mesoporous TiO₂ nanosponges, super-microporous silica, and conducting micro-silica spheres were prepared in ILs.^{17–20} Ni nanoparticles were synthesized in ILs via the thermolysis of nickel formate.²¹ M₂S₃ (M = Bi, Sn) nanorods were synthesized in an IL with ethylene glycol

[†] Department of Chemistry and Kanbar Laboratory for Nanomaterials at the Bar-Ilan University Center for Advanced Materials and Nanotechnology, Bar-Ilan University.

[‡] Department of Physics, Bar-Ilan University.

[§] The Hebrew University of Jerusalem.

- (1) Wang, X.; Zhuang, J.; Peng, Q.; Li, Y. *Nature* **2005**, *437*, 121.
- (2) Duan, X.; Huang, Y.; Cui, Y.; Wang, J.; Lieber, C. M. *Nature* **2001**, *409*, 66.
- (3) Iijima, S. *Nature* **1991**, *354*, 56.
- (4) Huynh, W. U.; Dittmer, J. J.; Alivisatos, A. P. *Science* **2002**, *295*, 2425.
- (5) Welton, T. *Chem. Rev.* **1999**, *99*, 2071.
- (6) Jain, N.; Kumar, A.; Chauhan, S.; Chauhan, S. M. S. *Tetrahedron* **2005**, *61*, 1015.
- (7) (a) Blanchard, L. A.; Hancu, D.; Beckman, E. J.; Brennecke, J. E. *Nature* **1999**, *399*, 28. (b) Cole-Hamilton, D. J. *Science* **2003**, *299* (5613), 1702.
- (8) (a) Endres, F.; Bukowski, M.; Hempelmann, H.; Natter, H. *Angew. Chem., Int. Ed.* **2003**, *42*, 3428. (b) El Abedin, S. Z.; Borissenko, N.; Endres, F. *Electrochem. Commun.* **2004**, *6*, 510.

- (9) Mu, X.; Evans, D. G.; Kou, Y. *Catal. Lett.* **2004**, *97*, 151.
- (10) Zhu, Y.; Wang, W.; Qi, R.; Hu, X. *Angew. Chem., Int. Ed.* **2004**, *43*, 1410.
- (11) Foneca, G. S.; Umpierre, A. P.; Fichtner, P. E. P.; Teixeira, S. R.; Dupont, Chem.—Eur. J. **2003**, *9*, 3263.
- (12) Firestone, M. A.; Dietz, D. L.; Seifert, S.; Trasobares, S.; Miller, D. J.; Zaluzec, N. J. *Small* **2005**, *7*, 754.
- (13) Wang, Y.; Yang, H. J. *Am. Chem. Soc.* **2005**, *127* (15), 5316.
- (14) Li, Z.; Zhang, J.; Du, J.; Gao, H.; Gao, Y.; Mu, T.; Han, B. *Mater. Lett.* **2005**, *59*, 963.
- (15) Wang, J.; Cao, J.; Fang, B.; Lu, P.; Deng, S.; Wang, H. *Mater. Lett.* **2005**, *59*, 1405.
- (16) Wang, W.; Zhu, Y. *Inorg. Chem. Commun.* **2004**, *7*, 1003.
- (17) Nakashima, T.; Kimizuka, N. *J. Am. Chem. Soc.* **2003**, *125*, 6386.
- (18) Zhou, Y.; Antonietti, M. *J. Am. Chem. Soc.* **2003**, *125*, 14960.
- (19) Zhou, Y.; Antonietti, M. *Adv. Mater.* **2003**, *15*, 1452.
- (20) Jacob, D. S.; Joseph, A.; Mallenahalli, S. P.; Shanmugam, S.; Makhiluf, S.; Calderon-Moreno, J.; Koltypin, Y.; Gedanken, A. *Angew. Chem., Int. Ed.* **2005**, *44* (40), 6560.

and ethanolamine.²² A PbO nanocrystal with a PbS-type structure was produced in an IL.²³ Recently, a large scale synthesis of single-crystal gold nanosheets has been reported in an IL without any additional template agent.²⁴

High-speed synthesis with microwave (MW) radiation has attracted a considerable amount of attention in recent years.²⁵ The efficient in-core volumetric heating with the help of MW radiation has helped to reduce chemical reaction times from hours to minutes, and it is also known to reduce side reactions, increase yields, and improve reproducibility.²⁶ The observed rate enhancement is a purely thermal/kinetic effect, that is, a consequence of the high reaction temperatures (because of the superheated solvents above their boiling temperature) that can rapidly be attained by irradiating polar materials in a MW field. The ionic nature and thermal stability of the RTIL make them very good solvents for absorbing MW radiation. This gives RTILs an advantage over other solvents in the synthesis of inorganic nanomaterials.^{10,22}

To explore the chemistry of ILs in the field of inorganic chemistry, we report herein on a fast and simple approach to the synthesis of a large variety of differently shaped nanocrystalline metallic fluorides using the combined effects of an IL as a solvent and MW heating. There are a few reports on the formation of metal fluorides under tribological conditions.²⁷ Traces of water and the presence of transition metal in ILs yield metal fluorides.¹¹ However, this phenomenon¹¹ was not observed for all the reactions carried out under MW irradiation, where the precursors have hydration water molecules, even if water was intentionally added to the reaction mixtures.^{10,15,16,24,28} Unlike ref 11, in all these cases fluoride was not obtained. It was also reported that the decomposition temperature of the IL was generally not affected, as a result of impurities (H₂O).²⁹ In the current article, our main focus is on the reactions of an IL, BMIBF₄, with different metal salts under MW radiation. This reaction is examined by changing the metal nitrates used, as well as by varying the irradiation time. In this paper, we concentrate on the synthesis of nanosized metal fluorides having different morphologies.

Experimental Section

Materials. 1-Butyl-3-methylimidazolium tetrafluoroborate (BMIBF₄, 99%, Solvent Innovation GmbH), iron nitrate (ACS Merck, 99%), cobalt nitrate (Riede de Haën, 97%), zinc nitrate, lanthanum nitrate, strontium nitrate, and yttrium oxide were purchased from Aldrich at concentrations $\geq 99\%$ and used in our reactions. Yttrium nitrate was synthesized by reacting yttrium oxide

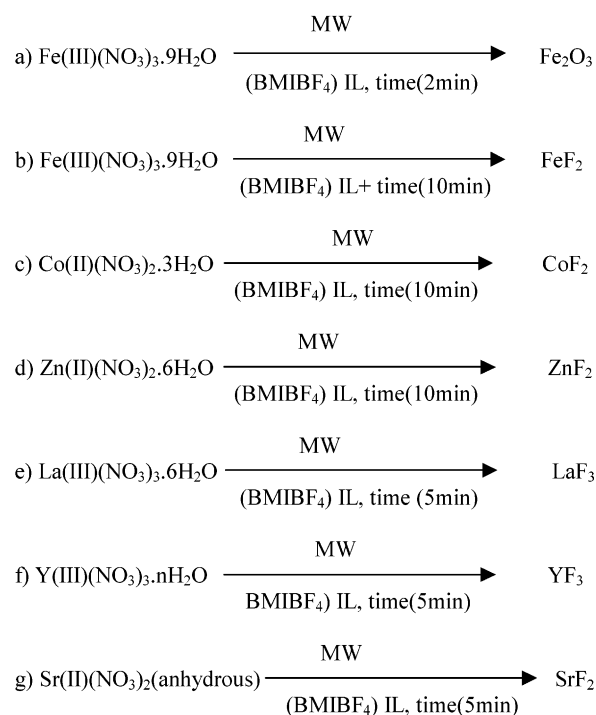
with concentrated nitric acid under heating. The crystalline product obtained was directly used for the synthesis of yttrium fluoride.

General Method of Synthesis. A BMIBF₄ (10 g for each reaction) IL solvent and metal precursor nitrate salts (1 g) in all the reaction systems were heated in a domestic microwave oven (2.45 GHz, Kenwood Microwave 900 W) at different time intervals. Herein, we give a general schematic representation (Scheme 1) for the formation of different fluorides at different time intervals with the same reaction conditions under MW irradiation. After completion of the reaction time the products were washed several times with acetone and ethanol to remove the IL and other organic impurities and centrifuged for 10 min at 9000 rpm. The washed products were dried under vacuum and used for further investigations. The quantitative yields of the products obtained after drying are in the range of 80–95% (with carbon as an impurity). The products were characterized by X-ray diffraction (XRD) measurements on a Rigaku X-ray diffractometer (model 2028, Co K α ; $\lambda = 1.788\ 92\ \text{\AA}$). The Mössbauer ⁵⁷Fe study was performed at ambient temperature using a conventional constant acceleration drive and a 50 mCi Co/Rh source. The experimental spectrum was analyzed by a least-squares fitting procedure, and the ⁵⁷Fe isomer shifts were relative to α -Fe. Raman spectra were recorded on a Jobin Yvon Horiba Raman System. The 524 nm line of an Ar⁺ laser was used as the excitation source. The structural morphology was studied with high-resolution transmission electron microscopy (HRTEM) on a JEOL-2010, using an accelerating voltage of 200 kV. Samples for HRTEM measurements were prepared by ultrasonically dispersing the products into absolute ethanol and then placing a drop of this suspension onto a copper grid coated with an amorphous carbon film and drying under air. High-resolution scanning electron microscopy (HRSEM) images were taken using a JEOL JSM-7000F field emission scanning electron microscope with an accelerating voltage of 15 kV.

Results and Discussion

XRD Results. All the XRD patterns of the products are presented in Figure 1, and in all the reactions we achieved

Scheme 1. Formation of Metal Fluoride and Metal Oxide in IL under MW Heating



(21) Zhang, S. M.; Zhang, C. L.; Wu, Z. S.; Zhang, Z. J.; Dang, H. X.; Liu, W. M.; Xue, Q. J. *Acta Chim. Sin.* **2004**, 62 (15), 1443.

(22) Jiang, J.; Zhu, Y. J. *Phys. Chem. B* **2005**, 109, 4361.

(23) Chen, L. J.; Zhang, S. M.; Wu, Z. S.; Zhang, Z. J.; Dang, Z. J. *Mater. Lett.* **2005**, 59, 3119.

(24) Li, Z. H.; Liu, Z. M.; Zhang, Z. L.; Han, B. X.; Du, J. M.; Gao, Y. N.; Jiang, T. J. *Phys. Chem. B* **2005**, 109 (30), 14445.

(25) Adam, D. *Nature* **2003**, 421, 571.

(26) Oliver Kappe, C. *Angew. Chem., Int. Ed.* **2004**, 43 (46), 6250.

(27) Liu, W. M.; Ye, C. F.; Gong, Q. Y.; Wang, H. Z.; Wang, P. *Tribol. Lett.* **2002**, 13 (2), 81.

(28) Jiang, Y.; Zhu, Y. *Chem. Lett.* **2004**, 33 (10), 1390.

(29) Fox, D. M.; Gilman, J. W.; De Long, H. C.; Trulove, P. C. *J. Chem. Thermodyn.* **2005**, 37, 900.

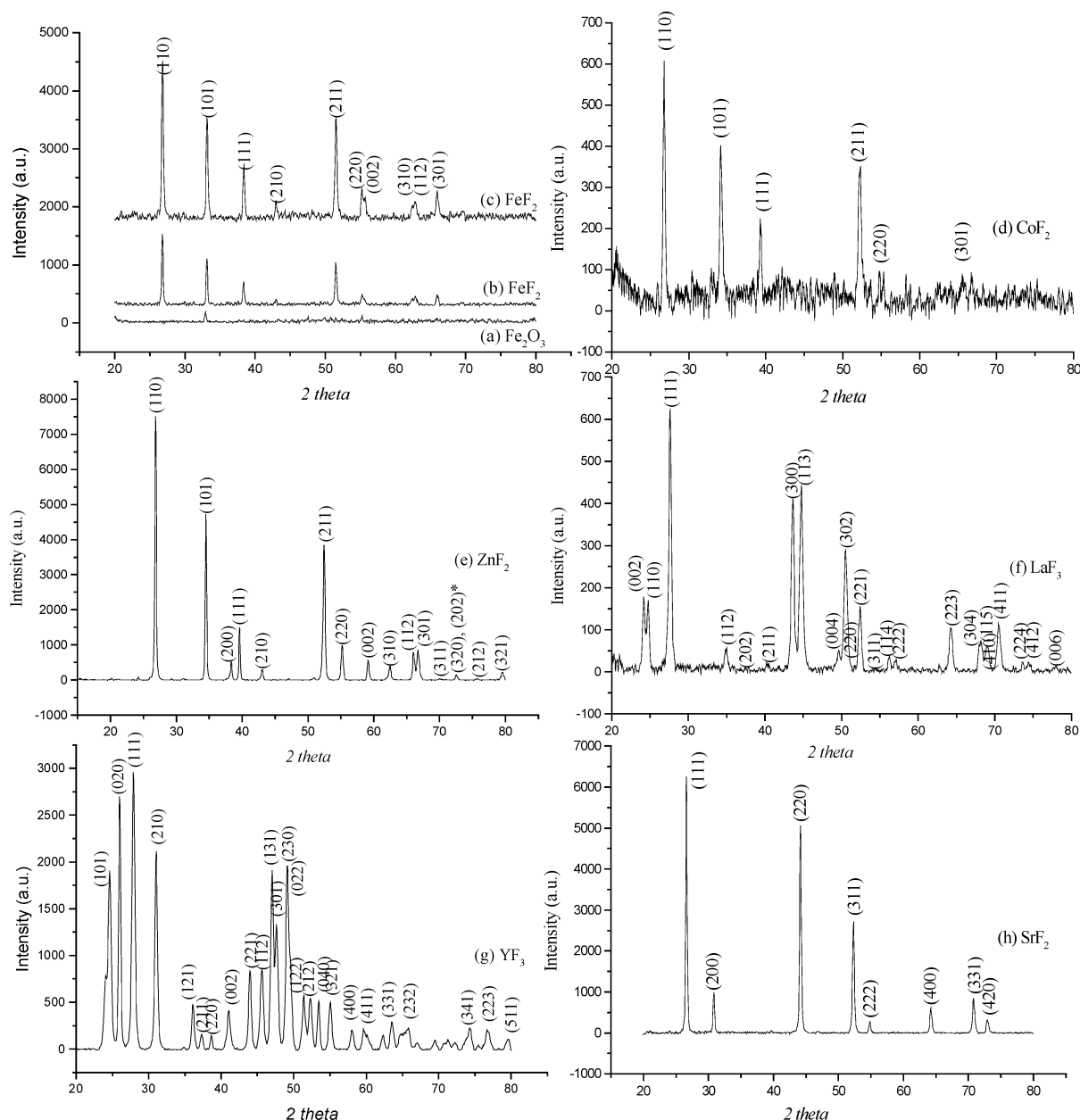


Figure 1. XRD patterns of synthesized products in IL under MW irradiation.

a single crystalline phase. The $\text{Fe}(\text{NO}_3)_3$ reaction yields Fe_2O_3 at a short reaction time (2 min) under MW irradiation in an RTIL. The XRD pattern of Figure 1a ($\text{Fe}(\text{NO}_3)_3$ as precursor) matches well the PDF-39-0238 (b, Fe_2O_3). The particle size calculated from the Scherrer equation ($d = k\lambda/(\beta \cos \theta)$) is ~ 30 nm (considering that the nanoparticles were spherical), which is comparable with the size of the particles measured from the HRTEM images. As the MW irradiation time is increased to 10 min for the $\text{Fe}(\text{NO}_3)_3$ precursor, FeF_2 is obtained as the sole product. The XRD patterns of the product obtained in a 10 min reaction of $\text{Fe}(\text{NO}_3)_3$ in a MW are shown in Figure 1b. These patterns match well with the PDF-45-1062 (tetragonal FeF_2). The reaction is also conducted in the presence of 10 wt % water (in addition to that of hydration water of the metal nitrates), and a 10 min MW reaction for the $\text{Fe}(\text{NO}_3)_3$ system in IL. The reason for the addition of water is to explore the effect of additional water on the morphology as well as on the products. We found

that the crystalline nature increases, as compared to products obtained without additional water, while the morphology also changes. The XRD pattern of the product, FeF_2 , under additional water is presented in Figure 1c. The MW reaction of $\text{Co}(\text{NO}_3)_2$ in IL produces CoF_2 for a short period reaction (5 min), as well as for a 10 min reaction. The XRD pattern of CoF_2 (10 min reaction) is shown in Figure 1d (PDF-01-071-0653, tetragonal). In this reaction we found that $\text{Co}(\text{NO}_3)_2$ in IL under MW irradiation is independent of the irradiation time, as we obtain the same product. However, from the XRD data we deduce that the product obtained from a 10 min reaction is more crystalline than that obtained from a short time reaction. The $\text{Zn}(\text{NO}_3)_2$ reaction in IL under MW irradiation for 10 min results in ZnF_2 . The XRD pattern is given in Figure 1e. The XRD pattern of the $\text{Zn}(\text{NO}_3)_2$ product matches well the PDF-1-89-5014, tetragonal ZnF_2 . The rare earth nitrate salt reactions in IL under MW irradiation gives well crystalline fluorides as products. A 5

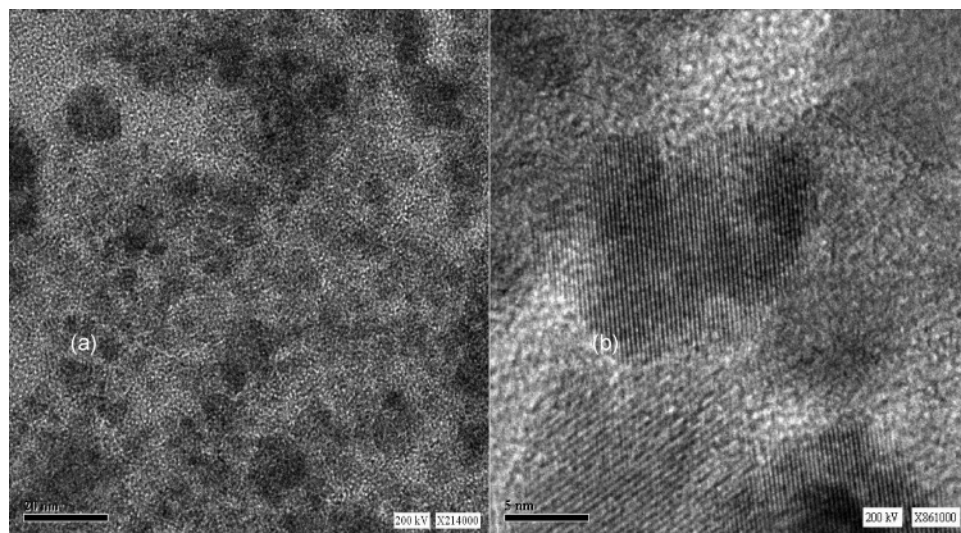


Figure 2. HRTEM images of Fe_2O_3 nanoparticles.

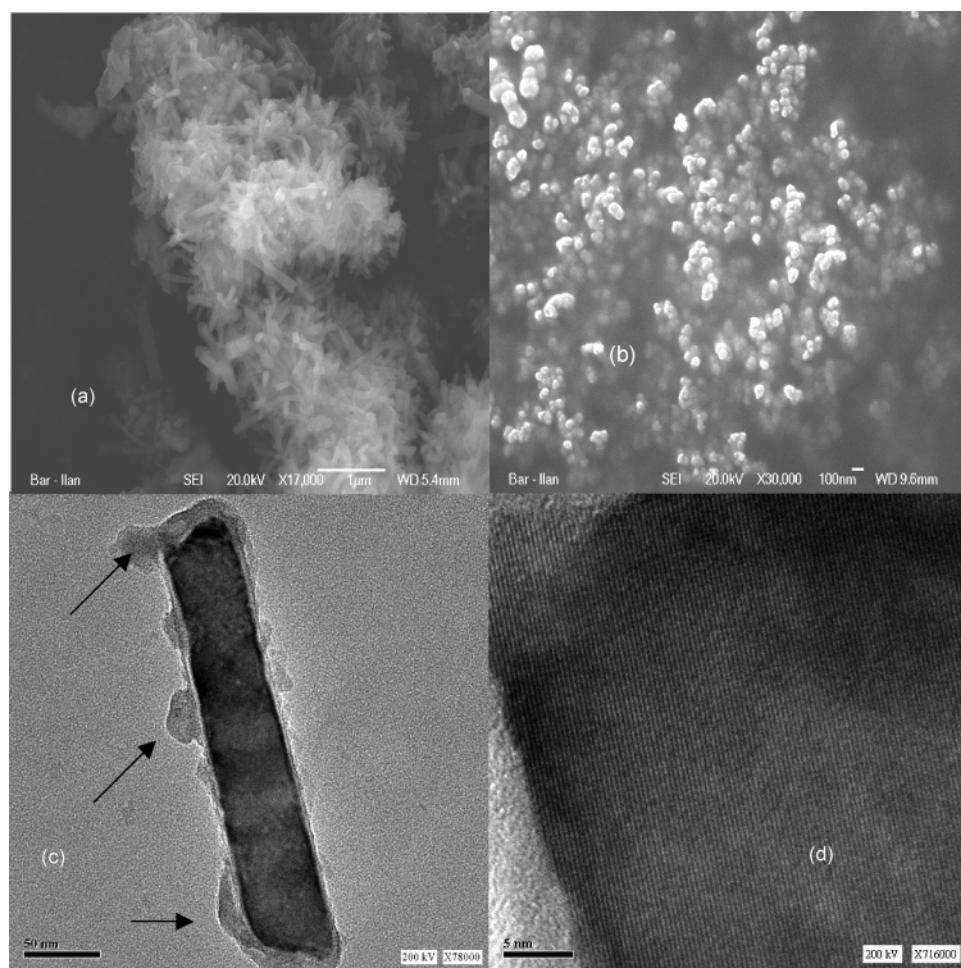


Figure 3. HRSEM for (a) bar shaped FeF_2 and (b) nanoparticles of FeF_2 and HRTEM (c, d) images of FeF_2 nanobars.

min MW irradiation was sufficient to obtain LaF_3 and YF_3 from the respective nitrate salts dissolved in IL. The XRD patterns of the products of the $\text{La}(\text{NO}_3)_3$ and $\text{Y}(\text{NO}_3)_3$ precursors are presented in Figure 1f,g, respectively. The XRD patterns are assigned to LaF_3 and YF_3 , based on a comparison with the XRD data of PDF-32-483 (hexagonal LaF_3) and PDF-1-70-1935 (orthorhombic YF_3), respectively. The $\text{Sr}(\text{NO}_3)_2$ reaction in IL under 5 min of MW irradiation

gives a crystalline SrF_2 product. The XRD pattern of the product is shown in Figure 1h and is in good agreement with PDF-006-0262, face-centered cubic SrF_2 .

Morphological Studies. HRTEM and HRSEM measurements were used to study the morphologies of the obtained products. A short 2 min MW irradiation of an $\text{Fe}(\text{NO}_3)_3$ precursor yields crystalline Fe_2O_3 nanoparticles, as shown by the X-ray pattern. The HRTEM images are shown in

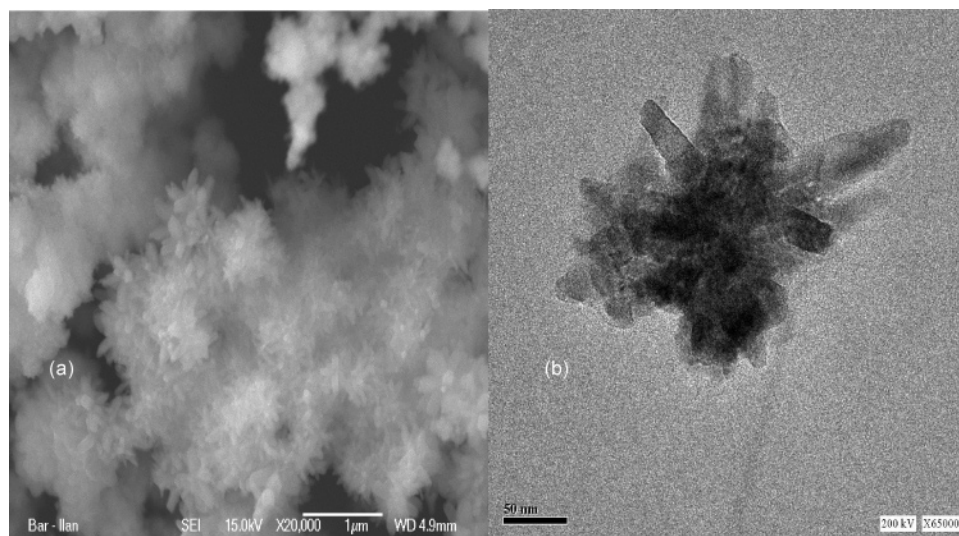


Figure 4. HRSEM (a) and HRTEM (b) images of CoF_2 aggregated needles.

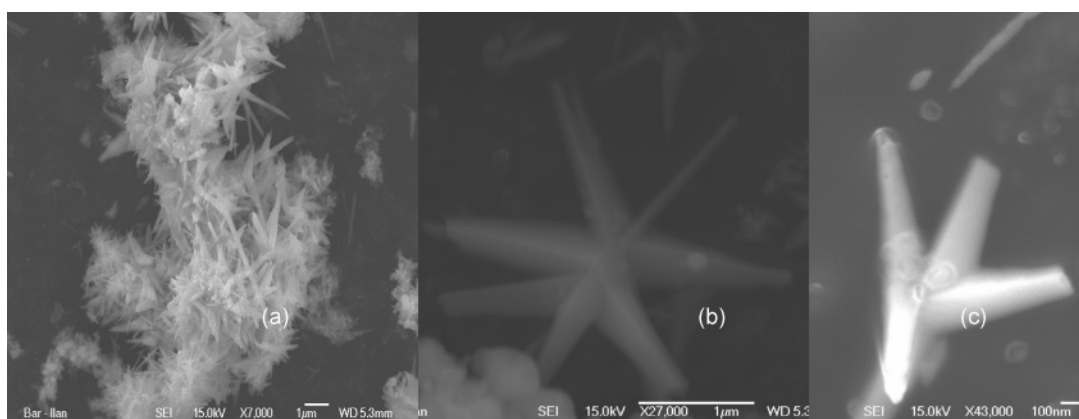


Figure 5. HRSEM images of the anisotropic nanostructure ZnF_2 .

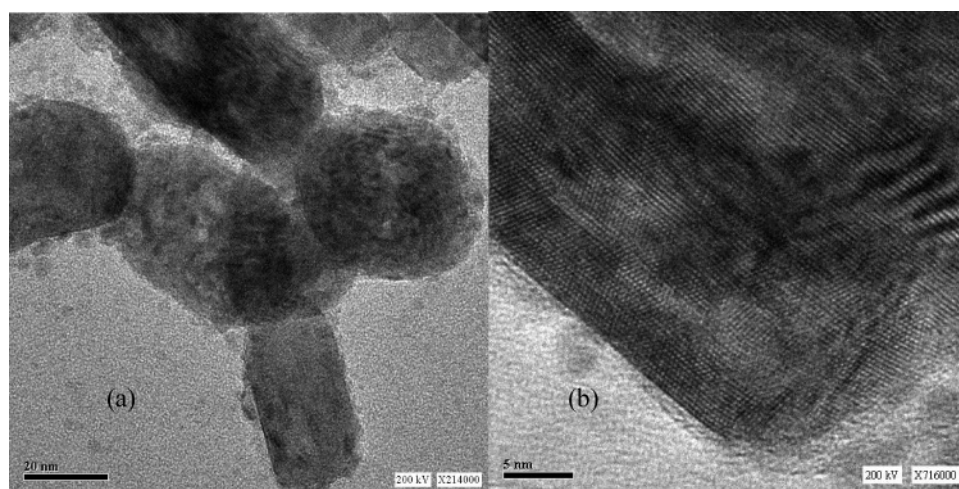


Figure 6. HRTEM images of oval shaped nanoparticles of LaF_3 .

Figure 2a,b. The single nanoparticles of Fe_2O_3 are in the range of 5–20 nm from the HRTEM images (Figure 2a,b). The observed spacing of the observed fringes is 2.7 \AA , fitting well with the d value of the (222) plane.

As the MW irradiation time is increased to 10 min for the above $\text{Fe}(\text{NO}_3)_3$ system, FeF_2 bars are obtained. The bar-shaped morphology of FeF_2 is seen in the HRSEM image in Figure 3a. The MW reaction carried out in the presence of additional water shows a morphological change. The bar-

shaped morphology is changed into nanoparticles of FeF_2 , as illustrated in the HRSEM image presented in Figure 3b. The HRTEM images for the bar-shaped FeF_2 are presented in Figure 3c,d. Figure 3d shows the fringes, whose spacing is 3.32 \AA , which also confirms the formation of crystalline FeF_2 . The HRTEM picture in Figure 3c shows the carbon wrapping the solid bar, as indicated by the small arrows. The carbon coating covers the whole FeF_2 bar.

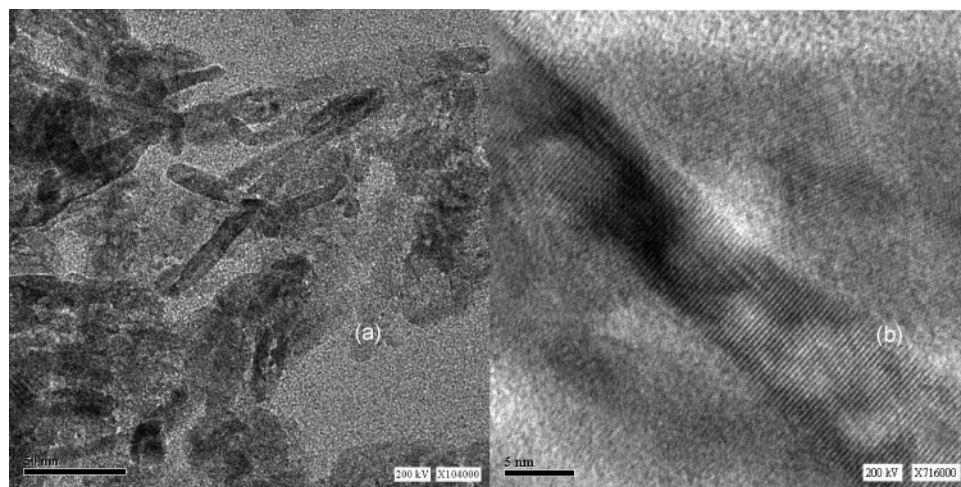


Figure 7. HRTEM images of needle shaped YF_3 nanoparticles.

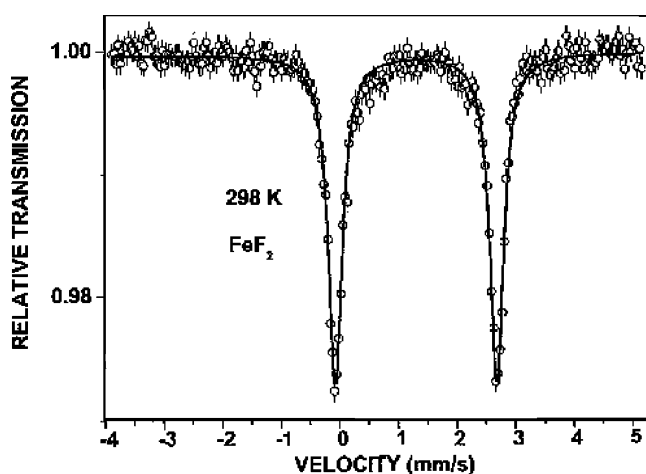


Figure 8. Mössbauer spectrum of FeF_2 synthesized in an IL under MW irradiation.

The reaction that $\text{Co}(\text{NO}_3)_2$ undergoes in an IL solvent under MW irradiation produces crystalline, aggregated needle-shaped CoF_2 . The aggregated needle structure of CoF_2 is presented in the HRSEM image in Figure 4a. Figure 4b presents an HRTEM image that shows the aggregated needle structure. The d spacing (3.32 \AA) obtained from the HRTEM image of the CoF_2 is analogous with the d value of the (110) plane.

Anisotropic structures are obtained for the $\text{Zn}(\text{NO}_3)_2$ nitrate system reacting with the IL under MW for a 10 min irradiation. The HRSEM images are shown in Figure 5a–c. For the $\text{Zn}(\text{NO}_3)_2$ system we found different morphologies of ZnF_2 such as bar, tripod, and star shapes.

A 5 min MW irradiation of $\text{La}(\text{NO}_3)_3$ and $\text{Y}(\text{NO}_3)_3$ salts in ILs gives well-dispersed nanocrystalline particles of the rare-earth fluorides, LaF_3 and YF_3 , respectively. The oval-shaped nanoparticles (LaF_3) and needle-shaped (YF_3) are shown in the HRTEM images, Figures 6 and 7. These products are crystalline and can be observed from the HRTEM images as well as from the XRD pattern.

Mössbauer and Raman Spectroscopy. A ^{57}Fe Mössbauer study at room temperature was performed for the FeF_2 bar shaped product by using a conventional constant acceleration drive and a 50 mCi $^{57}\text{Co}/\text{Rh}$ source. It is readily observed that the spectrum contains only one doublet and is presented

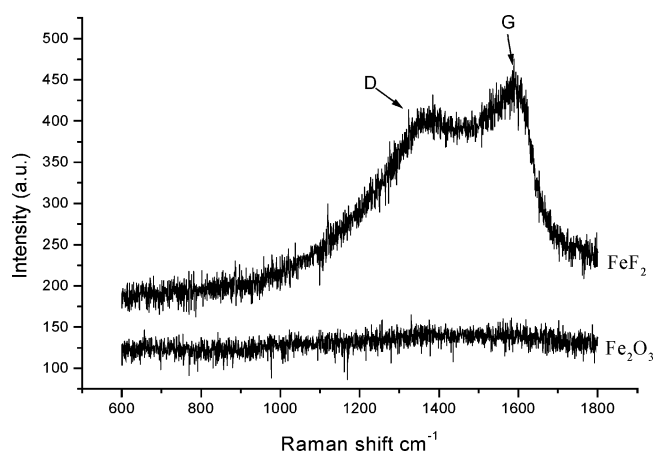


Figure 9. Raman spectra showing the presence of bands for carbon in FeF_2 that are absent in Fe_2O_3 , synthesized in IL under MW irradiation.

in Figure 8. A least-squares fit procedure yields the following values: isomer shift = $1.35(1) \text{ mm/s}$ (relative to $\alpha\text{-Fe}$), quadrupole splitting $1/2e^2qQ = 2.78(1) \text{ mm/s}$, and line width of $2.86(1) \text{ mm/s}$. These hyperfine parameters are identical to values published in the literature for FeF_2 .³⁰ The fact that a single doublet is observed indicates clearly (within a 3–5% limit of uncertainty) that the measured sample is a single phase material.

Raman studies have been carried out only for $\text{Fe}(\text{NO}_3)_3$ reactions in search of the reducing agent that yielded FeF_2 as the product. The Raman spectrum of a reaction product of $\text{Fe}(\text{NO}_3)_3$ in IL after 10 min of MW irradiation shows the two characteristic bands of carbon at 1354 cm^{-1} (D band) and at 1589 cm^{-1} (G band). The intensity of the G band related to the graphitic carbon is larger than the disordered D band carbon.³¹ These carbon bands are detected for the sample of bar-shaped FeF_2 . For the short reaction of 2 min of MW irradiation, no carbon peaks are detected. These results confirm that the Fe_2O_3 sample does not contain any type of carbon. Raman spectra are shown in Figure 9 for both FeF_2 and Fe_2O_3 samples. This also confirms that, during the 2 min reaction, no decomposition of the IL

(30) Greenwood, N. N.; Gibb, T. C. *Mössbauer Spectroscopy*; Chapman and Hall, Ltd.: London, 1971; p 117.

(31) Shanmugam, S.; Gedanken, A. *J. Phys. Chem. B* **2006**, *110*, 2037.

takes place. On the other hand, such dissociation occurs for the 10 min reaction. The carbon is the reducing agent for the Fe^{3+} ions.

In all above inorganic reactions conducted in IL solvents, the fabricated nanosized products were formed having different morphologies, that is, Fe_2O_3 (nanoparticles), FeF_2 (bars), CoF_2 (aggregated needle), ZnF_2 (anisotropic nanostructure), LaF_3 (oval), and YF_3 (needle-shaped). What is also common to all the current reactions is that the solvent, namely, the IL, serves as the source of the fluoride ions. In one case, that of the Fe(III) ions, where the Fe^{3+} was reduced to Fe^{2+} , the solvent was the source of the reducing agent. We have already argued that the IL is a good susceptor of the MW radiation because of its ionic nature. Therefore, its boiling temperature is reached within a very short time. When the (BMIBF_4) IL solvent exceeds its boiling temperature as a result of superheating, it decomposes. The BF_4^- anion undergoes fast hydrolysis in the presence of transition metal salts with hydration water molecules under MW superheating.^{11,29}



A similar $\text{BF}_3 \cdot \text{NH}_3$ is well-known.

This fluoride ion reacts with the metal, giving an insoluble metal fluoride. In parallel, the cation decomposes to form carbon. The formation of a small grain of carbon causes the temperature to further increase because of the thermal runaway phenomenon, which creates hot spots in the liquid.³³

In the $\text{Fe(NO}_3)_3$ system, for a short reaction time (2 min) MW radiation yields Fe_2O_3 because of the presence of oxygen in the air. At a longer reaction time, as the temperature rises, the decomposition of the imidazolium ion occurs, forming carbon. The hot carbon is the reducing agent that converts Fe(III) to Fe(II) .³⁴ The evidence for the formation of carbon is given above. In addition, we found

that C, H, N analysis shows a high concentration of carbon in the bar-shaped FeF_2 (7.1%) sample, as compared to other metal fluorides such as CoF_2 (2.4%) and ZnF_2 (4.2%). The solubility product of FeF_2 in the IL is smaller than that of FeO . The reaction of cobalt(II) nitrate with the IL forms CoF_2 in a very short (2 min) reaction time. This is because the reaction between Co^{2+} with F^- is fast. The same is true for almost all the other metal fluorides. The evidence for the existence of carbon, which plays an important role in the reduction of Fe^{3+} to Fe^{2+} , comes from HRTEM as well as from Raman spectroscopy. The HRTEM image is depicted in Figure 3c, where a layer of carbon is coating the FeF_2 bar. The Raman spectrum shows the presence of D and G bands for carbon in the FeF_2 sample. A ^{57}Fe Mössbauer study of the FeF_2 sample also reveals a single-phase material.

Conclusion

In conclusion, the answer to the question raised in the title is yes. ILs are a boon and are an important tool in the field of inorganic material synthesis. We have developed a simple general route for the synthesis of different nanosized morphologies of metal fluorides. What was common to all the metal fluorides was the one-dimensional rodlike structure. They differ, however, in the organization of the rods showing star-shaped, tripod, and aggregated needle morphologies, depending on the metal precursor. The Fe(III) system differed from the other systems, yielding Fe_2O_3 for a short reaction time, but for longer reaction times it forms a metal fluoride, FeF_2 . This synthesis method can be generalized for preparing metal fluorides in neutral IL under MW irradiation. We also have found some exceptional cases for metals such as copper, nickel, and silver nitrate systems in IL. Under similar reaction conditions pure metals are obtained. This will be reported elsewhere because our research is not complete.

CM060782G

(32) Gillespi, R. J.; Hartman, J. S. *Can. J. Chem.* **1967**, *45* (8), 859.

(33) Rao, K. J.; Vaidhyanathan, B.; Ganguli, M.; Ramakrishnan, P. A. *Chem. Mater.* **1999**, *11*, 882–895.

(34) (a) Kelly, R. M.; Rowson, N. A. *Miner. Eng.* **1995**, *8* (11), 1427–1438. (b) Zhong, S.; Geotzman, H. E.; Bleifuss, R. L. *Miner. Metall. Process.* **1996**, *13* (4), 174–178.